EJN European Journal of Neuroscience

FENS Federation of European Neuroscience Societies

European Journal of Neuroscience, pp. 1–12, 2017 doi:10.1111/ejn.13505

Stimulus-specific adaptation to visual but not auditory motion direction in the barn owl's optic tectum

Dante F. Wasmuht,[1] Jose L. Pena[2] and Yoram Gutfreund[1]

[1]Department of Neuroscience, The Ruth and Bruce Rappaport Faculty of Medicine and Research Institute, The Technion, Bat-Galim, Haifa 31096, Israel

[2]Dominick P. Purpura Department of Neuroscience, Albert Einstein College of Medicine, Bronx, NY, USA

Keywords: motion processing, multisensory, neuroethology, sound localization

Edited by Paul Bolam

Received 26 July 2016, revised 11 December 2016, accepted 12 December 2016

Abstract

Whether the auditory and visual systems use a similar coding strategy to represent motion direction is an open question. We investigated this question in the barn owl's optic tectum (OT) testing stimulus-specific adaptation (SSA) to the direction of motion. SSA, the reduction of the response to a repetitive stimulus that does not generalize to other stimuli, has been well established in OT neurons. SSA suggests a separate representation of the adapted stimulus in upstream pathways. So far, only SSA to static stimuli has been studied in the OT. Here, we examined adaptation to moving auditory and visual stimuli. SSA to motion direction was examined using repeated presentations of moving stimuli, occasionally switching motion to the opposite direction. Acoustic motion was either mimicked by varying binaural spatial cues or implemented in free field using a speaker array. While OT neurons displayed SSA to motion direction in visual space, neither stimulation paradigms elicited significant SSA to auditory motion direction. These findings show a qualitative difference in how auditory and visual motion is processed in the OT and support the existence of dedicated circuitry for representing motion direction in the early stages of visual but not the auditory system.

Introduction

Two alternative hypotheses have been proposed with regard to acoustic motion processing in the brain (Grantham, 1986; Middlebrooks & Green, 1991; Ingham *et al.*, 2001). The first hypothesis suggests that there is no dedicated auditory motion processing circuitry and that motion is encoded as a series of static locations. A prediction of this hypothesis, known as the snapshot hypothesis (Middlebrooks & Green, 1991), is that neural responses to motion are inseparable from neural responses to static stimuli. The alternative hypothesis is that the central auditory system contains neural circuitry dedicated to auditory motion processing, exclusively sensitive to parameters such as direction and velocity, as observed in the visual system (Newsome & Pare, 1988). It remains unclear which hypothesis reflects auditory motion processing in humans and other animals (Middlebrooks, 2015).

The waterfall aftereffect, a well-known psychophysical phenomenon, has been advocated as indication of a specialized neural representation of visual motion (Snowden & Freeman, 2004). In the waterfall aftereffect, a subject seeing motion in one direction for an extended period of time perceives objects moving in the opposite direction once motion is interrupted. This phenomenon can be explained by an explicit representation of motion direction in the brain undergoing adaptation (or fatigue) during prolonged viewing (Anstis *et al.*, 1998). Adaptation paradigms have been commonly used to uncover the independent coding of specific stimulus features, in psychophysical and brain imaging studies (Weigelt *et al.*, 2008).

In this paper, we applied adaptation paradigms, analogous to the waterfall effect, in the optic tectum (OT) of the barn owl to test whether OT neurons specifically adapt to a stimulus moving in one direction and hence respond more strongly to occasional stimuli moving in the opposite direction (i.e., display stimulus-specific adaptation (SSA) to motion direction). The OT, considered the homologue of the mammalian superior colliculus, contains aligned visual and auditory maps of space (Knudsen, 1982). Neurons in mid-layers of the OT display stimulus-specific adaptation (SSA) to features of visual and auditory stimuli such as location, frequency and intensity (Reches & Gutfreund, 2008; Netser *et al.*, 2011). The robust sensitivity to deviations from the common input is believed to reflect a tectal role in detecting salient stimuli (Gutfreund, 2012). However, SSA to moving stimuli has not been tested. To test this, we generated moving sounds using sweeps of binaural cues, interaural time (ITD) and level (ILD) difference, delivered through earphones and sequential activation of speakers at changing locations in a high-density speakers array. For comparison with responses to visual motion, moving visual stimuli were projected on a large screen in front of the owl. We found that OT neurons adapt

Correspondence: Yoram Gutfreund, as above.
E-mail: yoramg@tx.technion.ac.il

specifically to motion direction in visual but not auditory stimuli, demonstrating a difference in the way visual and auditory motion are represented in the OT. While visual motion appears processed in independent channels, auditory motion does not.

Materials and methods

Animals

Eight adult barn owls (*Tyto alba*) of both sexes were used in this study. All owls were hatched in captivity, and raised and kept in large flying cages. Five owls were used for auditory and visual experiments in the Technion and three owls for free-field auditory stimulation at the Albert Einstein College of Medicine. The owls were provided for in accordance with the guidelines established by the NIH on the care and use of animals in research. All procedures were approved by the Technion Institutional Animal Care and Use Committee and the Albert Einstein College of Medicine Institute of Animal studies.

Electrophysiology

Electrophysiological experiments were performed in two separate laboratories, in one laboratory the responses to dichotic stimuli as well as visual stimuli were measured, in the other laboratory the responses to free-field auditory stimuli were performed. Therefore, some differences in the experimental procedures exist. For the dichotic and visual experiments: Owls were prepared for repeated electrophysiological experiments in a single surgical procedure. A craniotomy was performed and a recording chamber was cemented to the skull. Owls were food deprived 12 h before recording. At the beginning of each recording session, the owl was anesthetized briefly using isoflurane (2%) and nitrous oxide in oxygen (4:5) for positioning in a custom-made stereotaxic device at the center of a double wall sound-attenuating chamber (internal size – $2 \times 2 \times 2$ m) lined with echo suppressing foam. During the experiment, the isoflurane was removed and the bird maintained on a fixed mixture of nitrous oxide and oxygen (4:5). The head was aligned using retinal landmarks (Gold & Knudsen, 2000). A glass-coated tungsten microelectrode (1 MΩ; Alpha Omega, Nazareth, Israel) was driven into the recording chamber using a motorized manipulator (SM-191; Narishige, Tokyo, Japan). The recorded electrical signals were amplified, digitized, filtered (313–5000 Hz) and stored using the AlphaLab SnR system (Alpha Omega, Nazareth, Israel). In each experiment, a threshold was set online to select the larger units in the recording sites isolating action potentials from a small cluster of neurons (multi-unit recording). If a clear large single unit was identified in the recordings, the threshold level was set to isolate it. Data points corresponding to single units are specifically identified in the figures. We did not observe major differences between single and multi-unit results, therefore single and multi-unit recordings were analyzed together.

For experiments in the free-field setup, anesthesia consisted of intramuscular injections of ketamine hydrochloride (20 mg/kg; Ketaset) and xylazine (4 mg/kg; Anased). Prophylactic antibiotics (ampicillin; 20 mg/kg, i.m.) and lactated Ringer's solution (10 mL, s.c.) were administered at the beginning of each experiment. The depth of anesthesia was monitored by pedal reflex. Additional injections were given to maintain anesthesia during the experiment. To control for varying levels of anesthesia, records of the time of each recording relative to anesthetic administration were rigorously maintained. Experiments were interrupted when latencies or response thresholds changed. Body temperature was maintained throughout the session with a heating pad. Single-unit responses were recorded using 1 MΩ tungsten electrodes (A-M Systems). OT was located stereotaxically and confirmed by the characteristic bursting activity and spatially restricted visual and auditory RFs (Knudsen, 1982). Position within the OT was determined based on the location of the RFs. Once an OT unit was isolated and identified, earphones were removed for sound stimulation in free field.

At the end of each session, the recording chamber was treated with chloramphenicol 5% ointment and closed. An intramuscular injection of carprofen (3 mg/kg, Rimadyl) was given as analgesic. Owls were allowed to recuperate in their home cages for at least 7 days before the next session.

Auditory Stimulation

Auditory stimuli were synthesized on a PC connected to a Tucker-Davies Technologies (TDT) system III (40 KHz sampling rate; 24 bit D/A) running custom Matlab programs. For dichotic stimulation, computer-generated signals were transduced by a pair of matched miniature earphones (ED-1914; Knowles, Itasca, IL, USA). The earphones were placed in the center of the ear canal, about 8 mm from the tympanic membrane. The amplitude and phase spectra of the earphones were equalized within ±2 dB and ±2 μs between 2 and 12 kHz by computer adjustment of the stimulus waveform. Sound level was controlled by two independent attenuators (PA5; Tucker-Davis Technologies) and is reported as average binaural sound intensity (ABI) relative to a fixed sound pressure level of ~90 dB SPL measured 1 mm from the speaker. Stationary stimuli consisting of broadband (2–12 kHz) 50 ms sound burst with rise/fall times of 5 ms, presented at an inter-stimulus interval (ISI) of 1 s were used to map RFs and obtain ITD and ILD tuning curves of tectal neurons (Fig. 1B). Tuning curves were generated by varying a single parameter (ITD or ILD) while holding all other parameters constant. The tested parameter was varied randomly in stimulus sets that were repeated 10–20 times. The width of tuning curves was defined as the ITD or ILD range over which responses were 50% of the maximal response; best ITD or ILD was the midpoint of this range. To induce an ITD sweep, a varying time delay was introduced to one ear while maintaining the phase of the other ear constant. ITD was varied ± 100 μs around the site's best ITD. For creating stationary ILDs, the value of each of the two attenuators was controlled directly in each trial. To synthesize sweeps in ILD, sound levels on each side were adjusted by:

$$v_r(t) = 10\left(\frac{\mathrm{sir}(t)}{20}\right); v_l(t) = 10\left(\frac{\mathrm{sil}(t)}{20}\right)$$

where V_r and V_l are the amplitudes in volts, fed to the right and left attenuator, respectively and sir(t) and sil(t) the desired sound intensity sweeps in dB relative to the average ABI, for the right and left ears, respectively. In our experiments, *sir* and *sil* were reciprocal linear sweeps, i.e., one ear moving from 20 dB below to 20 dB above the ABI and the other in the opposite direction, creating a linear ILD sweep between ±40 dB. The total stimulus duration was adjusted to create the desired velocity. To transform ITD values to corresponding azimuthal locations, we used a calibration equation reported for barn owls (Brainard & Knudsen, 1993): ITD (in μs) = 2.5 * azimuth (in degrees).

Free-field stimuli were delivered using a custom-made hemispherical array of 144 speakers (Sennheiser, 3P127A) constructed inside

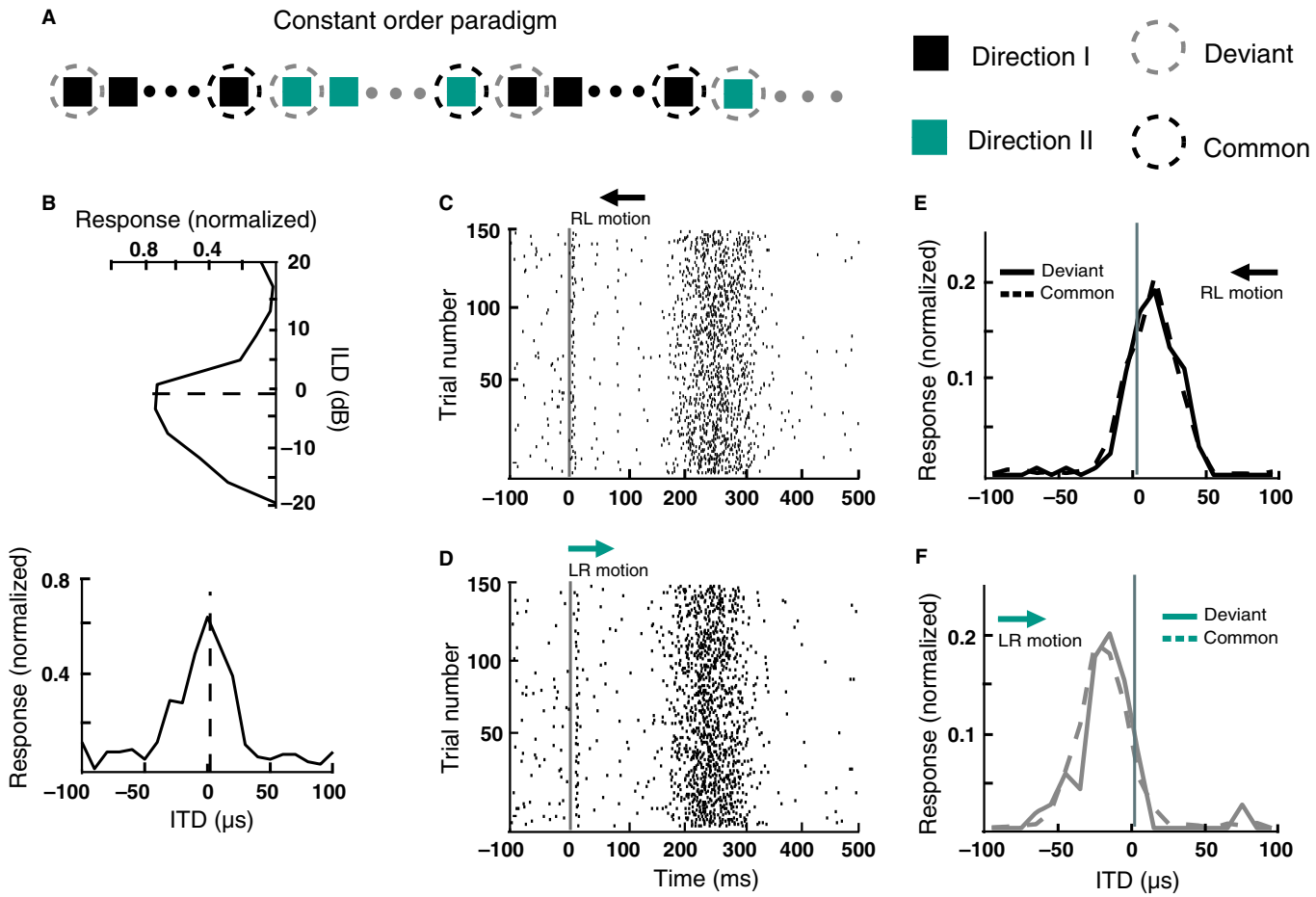

FIG. 1. Experimental paradigm and example response to ITD sweeps. (A) Constant order paradigm. Blocks consist of sweeps in one direction (black squares), switching to the opposite direction every 15 trials (gray squares). The response to the first stimulus after the switch (deviant, gray dashed circle), was compared with the response to the last stimulus before the switch (common, black circle). (B) ITD and ILD tuning curves for the recording site. The ILD curve is plotted on an orthogonal axis to emphasize that ILD is a cue for vertical position. Dashed lines indicate the preferred ITD and ILD. (C and D) Raster plots of spiking responses to two stimuli, right to left motion (RL; black arrow, panel C) or left to right motion (LR; gray arrow; panel D). Each row represents one trial. For each direction, 150 trials were presented (y-axis). The gray solid line indicates the motion onset. Directions were alternated every 15 sweeps. (E and F) Dynamic ITD tuning curves (averaged across trials) for each motion direction. The x-axis represents instantaneous ITD at corresponding times during motion. The solid lines represent the response to the deviant stimulus (first response after switching direction). The dashed lines represent the response to the common stimulus (average of responses to the last three stimuli in a block). Arrows indicate motion direction (black for RL motion and gray for LR motion). Vertical gray lines indicate the best-ITD for this recording site measured with static stimuli.

a sound-attenuating chamber (Perez *et al.*, 2009; Wang *et al.*, 2012). The speaker array ranged ±100 deg in azimuth and ±80 deg in elevation. The angular separation between the speakers varied from 10 deg to 30 deg. The highest density of speakers was located at the center of the array (40 deg around origin) and on the vertical midline and horizontal dimension at zero elevation. Each speaker in the array was calibrated using a Bruel and Kjær microphone (model 4190). Spatial tuning was assessed with broadband (0.5–10 kHz) sound bursts, 100 ms in duration, presented at random locations within the speaker array. Up and down-ramps for each burst were 5 ms and the ISI was 500 ms (offset-to-onset). Forty-five to 50 trials were tested for each speaker location. Each unit's preferred location was defined as the midpoint of the spatial locations that elicited responses equal or larger than half the maximum. After a site's preferred location was determined, the owl was rotated so the center of the site's spatial receptive field (SRF) was horizontally aligned with the center of the speaker array. The SRF mapping was repeated with the owl in the new orientation and subsequent free-field tests were performed in this condition. Motion was initiated either horizontally or vertically, ranging 40 degrees around the SRF center. Broadband, 120 ms sound bursts with 40 ms ramping were presented in sequence across the array. Onset and offset ramps of adjacent speakers overlapped 60 ms in time to create a perceptually smooth motion. The duration of each motion sweep was 500 ms for an 80 deg displacement, corresponding to a velocity of 160 deg/s, followed by 1-s ISI (offset-to-onset).

Visual stimulation

Visual stimuli were synthesized on a PC running custom Matlab programs with Psychtoolbox extension (Brainard, 1997). The visual scene was projected from outside the sound-attenuating chamber through a double-glass window on a wide screen (170 × 170 cm, 1.5 meters away from the animal) inside the chamber. The visual stimulus was a dark dot (about 1 deg in diameter) presented on a gray background. Luminance of dots was 8–12 cd/m^2 and luminance of background screen was 17 cd/m^2. The receptive field (RF) in visual space was estimated by varying the azimuth and the

elevation of the dot projected on the screen. For motion stimuli, the dot was made to move across the entire screen (corresponding to 60 deg in azimuth and 60 deg in elevation) crossing the RF at a fixed azimuth or elevation. Duration of motion was 500 ms, 1 s or 2 s, corresponding to velocities of about 120 deg/s, 60 deg/s and 30 deg/s, respectively. Each motion sweep was followed by 1s ISI. As eye movements in barn owls are limited to a range that is smaller than ±2 deg, (du Lac & Knudsen, 1990), we did not immobilize or control for eye movements.

Measurement of stimulus-specific adaptation

For each test, be it visual or auditory motion, two opposite motion directions, either left to right and right to left or upward and downward, were presented. The two motion stimuli could be either following exactly the same path but in opposite directions or two parallel paths in opposite directions (see insets in Fig. 2). In the first case, the sweep passed through the preferred ITD and ILD or center of the SRF. In the second case, the two paths differed in ITD or ILD, or crossed the SRF at equidistant points from the center. In all cases, motion trajectories passed through the excitatory regions of the neurons' RFs. Two stimulation paradigms were used to measure SSA: (1) In the constant order paradigm (Fig. 1A), one motion direction was repeated 15 times and subsequently followed by 15 sweeps in the opposite direction. This was repeated for 11 times, so that the total number of trials was 330 (165 for each direction). Each 15-trial set of sounds moving in the same direction was called a block. For visual stimulation, blocks consisted of 10 sweeps, resulting in 220 trials in total (110 for each direction). In all cases, the first two blocks were not included in the analysis to avoid onset effects (Reches & Gutfreund, 2008). The first presentation of a stimulus within a block was regarded as the deviant stimulus, because it was different from its immediate past. The average response of the last three stimuli within a block was used to assess the response to the common stimulus. (2) In the oddball paradigm, which was tested only with dichotic stimuli, the two selected motion directions were presented randomly, in a probabilistic manner. One of the stimuli was defined as the deviant and the other as the common stimulus (Fig. 3A). Each experimental block of this paradigm consisted of 150 stimuli, where the probability of occurrence was 90% for the common stimulus and 10% for the deviant. In the next experimental block, the directions of the common and deviant stimuli were reversed. This allowed to compare the average neural response to a moving stimulus when deviant, with the average response to the same stimulus when common. To prevent onset effects, each block was preceded by 15 repetitions of the common stimulus that were not included in the analysis.

Data analysis

For each stimulus in a sequence, responses were defined as the number of spikes in a time window starting at the onset of stimulus motion minus the number of spikes in a corresponding time window immediately before stimulus onset. The time window for spike count was either, 500 ms, 1000 ms or 2000 ms, corresponding to the stimulus duration. For each test, average responses were obtained for four conditions: direction 1 common (S_1c), direction 1 deviant (S_1d), direction 2 common (S_2c) and direction 2 deviant (S_2d). To quantify the SSA effect, we used the indices defined by Ulanovsky *et al.* (2003). The stimulus index (SI) is the normalized difference between the mean response to the deviant stimulus and the mean response to the common stimulus, defined as:

$$\mathrm{SI} = \frac{S_i d - S_i c}{S_i d + S_i c}$$

To analyze the population tendency for SSA, the SI measured in one direction was plotted against the SI measured in the other direction for each recording site (see for example Fig. 2B and D). Data points within the top-right quadrant (indicated by dashed lines) are stronger responses to the first deviant for both directions. However, as pointed by Ulanovsky *et al.*, (2003), any point above the diagonal line implies SSA, for the following reason: If the adaptation is not stimulus-specific and the SI for one direction is larger than zero, then the SI for the other direction is expected to be smaller than zero by the same amount (for a mathematical validation of this statement see Ulanovsky *et al.*, 2003)., i.e., the points are expected to be on the diagonal line. Thus, significant skewness of the points in the SI scattergram above the diagonal line is a widely accepted criterion for SSA at the population level (Reches & Gutfreund, 2008; Malmierca *et al.*, 2009; Taaseh *et al.*, 2011).

Population averages were obtained by normalizing each recording site by the maximum response and computing the mean across all sites.

Results

This study analyzed responses from 510 recording sites in the OT. In total, 362 sites were recorded from five owls at the Technion (recording sites per owl: 96, 85, 23, 67 and 91) and 149 sites were recorded from three owls at the Albert Einstein College of medicine (recording sites per owl: 31, 60, 58). No apparent differences between owls were observed, therefore, for population analysis, recording sites were pooled across owls. All sites were below the superficial bursting layer of the OT, which is the region where both visual and auditory responses have been reported (intermediate/deep layers; Ramon y Cajal layers-11-14 (Knudsen, 1982; Netser *et al.*, 2010)).

SSA to motion direction in ITD and ILD sweeps

In barn owls, ITD constitutes the main auditory localization cue for azimuth while ILD is the main cue for elevation due to the asymmetrical morphology of the ears (Moiseff, 1989). SSA to the direction of ITD sweeps was first studied using a constant order paradigm (see Materials and Methods). In the example shown in Fig. 1, best ITD was 0 μs and best ILD was −1 dB (Fig. 1B). In this experiment, an ITD sweep was presented repeatedly, switching its direction (from left ear leading to right ear leading) every 15 trials. The sweep velocity was 400 μs/s (corresponding to about 160 deg/s) and the ILD was fixed at the best ILD of the site. As the stimulus sweeps through the RF, the firing rate increases in both the leftward (Fig. 1C) and rightward (Fig. 1D) directions. Two rate-ITD curves were computed for each direction, from the average responses to the first trial after the switch (solid lines in Fig. 1E and F) and the average response to the last three trials before switching direction (dashed lines in Fig. 1E and F). In both directions, the curves for first and last trials were similar, suggesting a lack of SSA. However, the curves peak for leftward motion was shifted rightward from the 0 μs best ITD (Fig. 1E), while the peak for the rightward movement was shifted leftward (Fig. 1F). The shift in best ITD in the direction of the incoming sweep is consistent with a previous report (Witten *et al.*, 2006).

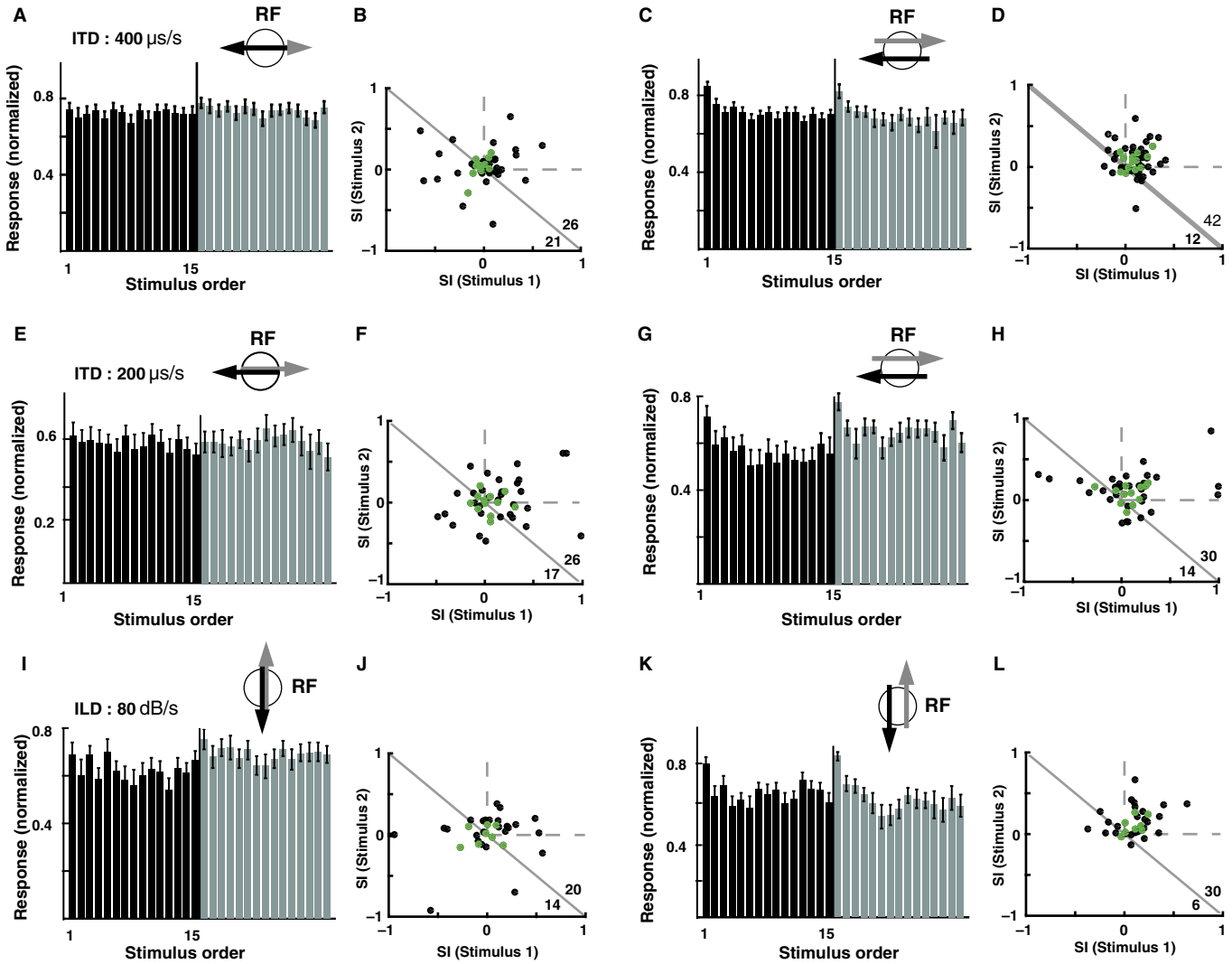

FIG. 2. Summary of results from the constant order paradigm. (A) Responses to ITD sweeps at 400 µs/s. Histogram of average responses to moving stimuli as a function of the order of the stimulus within the sequence. The first 15 black bars present responses to leftward motion and the last 15 gray bars to rightward motion. Error bars represent SEMs. In these experiments, the paths in both directions overlapped in ITD-ILD space, passing through the center of the RF (illustrated in the inset). (B) Stimulus indices (SIs) for one ITD-sweep direction plotted vs. SIs for the opposite direction. The dashed lines represent the upper right quadrant where both SIs are positive. Gray dots represent results from single-unit recordings, black dots from multi-unit recordings. The number of points above and below the diagonal line are shown in the bottom right corner. (C and D) Responses to ITD sweeps (400 µs/s) and SI plots, where motion paths in each direction differed in ILD, passing through opposite sides of the RF (illustrated in the inset). Same format as in A and B. (E and F) Responses to ITD sweeps at (200 µs/s, through the center of the RF. Same format as in A and B. G and H) Responses to ITD sweeps (200 µs/s), along two parallel paths (different ILD). Same format as in A and B. (I and J) Responses to ILD sweeps (80 dB/s), in opposite directions through the center of the RF. Same format as in A and B. K and L) Responses to ILD sweeps (80 dB/s), in opposite directions along parallel paths (different ITD). Same format as in A and B.

Across the sample, the average response to the first stimulus after switching directions was not significantly different from the average response to the last three stimuli of each block (Fig. 2A; $n = 47$, Wilcoxon signed rank test, $P = 0.06$ and $P = 0.59$ for right to left and left to right motion, respectively). Consistently, stimulus indices (SIs) were not significantly distributed above the diagonal line (Fig. 2B; sign test, $P = 0.56$). Thus, there was no significant SSA at the population level.

It is known from other systems that SSA can be sensitive to stimulus duration, inter-stimulus interval, probability of occurrence and stimulation paradigm (Ulanovsky *et al.*, 2004; Malmierca *et al.*, 2009). To rule out the possibility that the absence of SSA might be due to the specific stimulus timings used (a 500 ms duration stimulus and 1-s ISI, repeated 15 times before switching to the other direction), we performed an additional SSA test in each recording site. In this control test, the same paradigm and stimulus conditions were used but in addition to a change in direction, the two stimuli differed in ILD by 10–20 dB, depending on the width of the ILD tuning curve. Tectal neurons in the intermediate/deep layers are known for their SSA to both ILD and ITD (Reches & Gutfreund, 2008). Therefore, if SSA is observed when the two stimuli differ in ILD, it demonstrates that the stimulus paradigm is adequate for exposing SSA. Indeed, when the ILD of the two stimuli differed, clear SSA emerged (Fig. 2C, D). The first stimulus in both directions elicited significantly larger responses compared to the last presentations (Fig. 2C; $n = 54$, Wilcoxon signed rank test, $P < 0.001$ and $P < 0.001$, for right to left and left to right motion, respectively). Consistently, the majority of data points in the scatterplot of

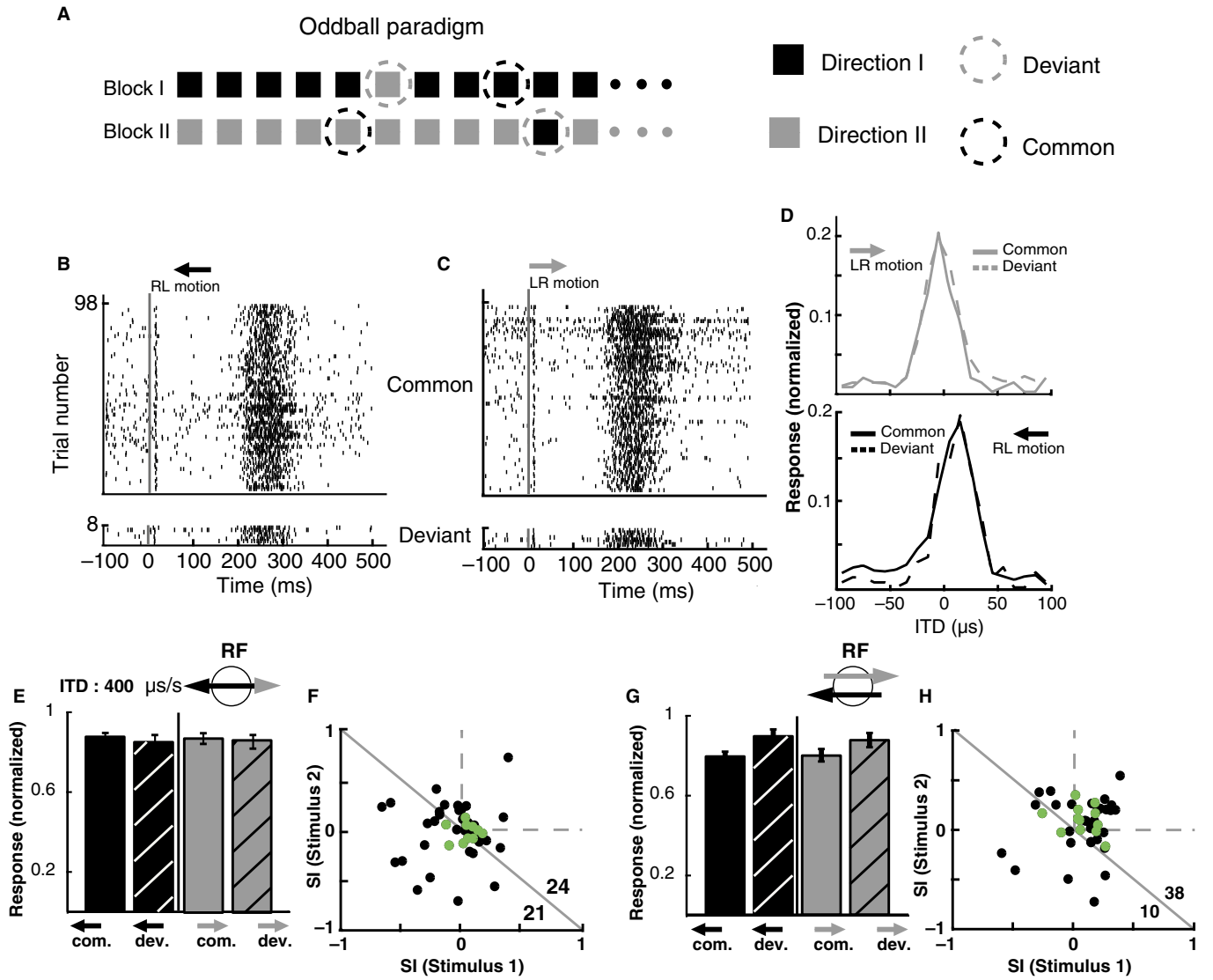

FIG. 3. Responses to the oddball paradigm. (A) A scheme illustrating the oddball paradigm. (B) Oddball paradigm. A sound moving in one direction (black squares) is presented randomly but more frequently (90% probability) than the opposite direction (10%, gray squares). In successive blocks, the probabilities are switched, the common direction in the previous block becomes rare and vice versa. (B) Example raster plots of responses to right to left (RL) motion when common (top) and deviant (bottom). Gray vertical line indicates the onset of the stimulus. (C) Responses for the same neuron in A to left to right (LR) motion when common (top) and deviant (bottom). (D) Dynamic ITD tuning curves calculated from the responses shown in B and C. Top shows tuning curves for LR motion, solid line when common and dashed line when deviant. Bottom shows tuning curves for RL motion. (E) Average responses across the sample. Bars represent responses to common and deviant stimuli for RL (black bars) and LR (gray bars) directions. Error bars represent SEM. (F) SIs scatterplots for one direction vs. the other. The dashed lines indicate the upper right quadrant. Gray dots represent results from single-unit recordings, black dots from multi-unit recordings. The number of points above and below the diagonal are shown on the lower right corner. (G and H) Average results from the oddball experiments where the ITD sweeps in opposite directions also differed in ILD. Format as in E and F.

SI1 vs. SI2 were above the diagonal line (Fig. 2D; sign test, $P = 0.00005$). This shows that the motion paradigm used here is capable of exposing SSA.

In the above experiments, the velocity of motion was 400 μs/s, which corresponds in barn owls to roughly 160 deg/s azimuthal velocity. For a flying predator, like the barn owl, the ethologically relevant acoustic speeds can vary dramatically depending on the distance to the source as well as self-motion. Head rotations in barn owls can reach 800 deg/s (du Lac & Knudsen, 1990), while a running mouse at a distance of about 1 meter can induce motion cues of 30 to 90 deg/s (50–150 cm/s). Thus, the acoustic velocity used here is expected to be ethologically relevant for barn owls. However, to verify that the lack of SSA to motion direction was not restricted to a specific velocity, we performed the test using an additional velocity of 200 μs/s (corresponding to about 80 deg/s, $n = 43$). The result was qualitatively similar to the result obtained using the faster velocity. The population average response to the first stimulus, in each block, was not different from the population average response to the last three stimuli (Fig. 2E, n = 43, Wilcoxon signed rank test, $P = 0.12$ and $P = 0.76$, for right to left and left to right motion, respectively) suggesting absence of SSA. However, when the ILD of the sounds moving in each direction differed by 10–20 dB, the population average response to the first stimulus in each sequence was again significantly larger than the responses at the end of the block (Fig. 2G; $n = 44$, Wilcoxon signed rank test, $P = 0.01$ and $P < 0.001$). These results indicate

that for the slower velocities as well, SSA to motion direction was not observed.

Next, we examined responses to ILD sweeps (mimicking up and down motion for the owl). We first used a constant order paradigm, where ILD was swept 20 dBs in opposite directions while ITD was fixed at the preferred value of the recording site (inset in Fig. 2I). The ILD sweep velocity was 80 dB/s, corresponding roughly to 120 deg/s (Olsen *et al.*, 1989; Poganiatz & Wagner, 2001). Similar to the results obtained with ITD sweeps, significant SSA was not observed; the response to the first stimulus in the sequence was not significantly different from the response to the last three stimuli (Fig. 2I–J $n = 34$, Wilcoxon signed rank test, $P = 0.47$ and $P = 0.08$, for downward and upward motion, respectively). The SI distribution was not significantly above the diagonal line (Fig. 2J; sign test, $P = 0.394$). However, clear and significant SSA was observed when stimuli in each direction differed also in ITD (Fig. 2K; ΔITD = 30–80 μs, $n = 36$, Wilcoxon signed rank test, $P < 0.001$ and $P < 0.001$). Consistently, the SIs were significantly distributed above the diagonal (Fig. 2K; sign test, $P = 0.00007$). The above results indicate that tectal neurons tend not to show SSA to the direction of ITD or ILD sweeps.

A caveat of using the constant order paradigm for testing SSA is that both stimuli are presented in equal numbers over a longer time-scale and hence, long-term non-specific adaptation may reduce SSA (Ulanovsky *et al.*, 2004). To verify that the absence of SSA to the direction of motion is not due to the constant order paradigm, we performed a probabilistic oddball test, where the probability of occurrence of the deviant stimulus was 10% (see Material and Methods). This oddball paradigm also failed to elicit SSA (Fig. 3). The average response over the sample was not significantly different between the deviant and the common condition (Fig. 3E, $n = 45$, Wilcoxon signed rank test, $P = 0.90$ and $P = 0.64$ for right to left and left to right motion, respectively); the scatterplot of SI1 vs. SI2 was not significantly shifted with respect to the diagonal line (Fig. 3F; sign test, $P = 0.766$). However, as expected, SSA emerged when both moving stimuli differed also in ILD (Fig. 3G and H; $n = 48$, Wilcoxon signed rank test, $P = 0.003$ and $P = 0.02$, sign test, $P = 6.17e\text{-}05$).

SSA to motion direction in free field

While the above experiments used ITD and ILD sweeps as a proxy for sound motion, real auditory motion may involve a combination of binaural and spectral cues that correlate with direction (Keller *et al.*, 1998; Poganiatz *et al.*, 2001; Cazettes *et al.*, 2014). To account for a more naturalistic set of cues, we also tested SSA to the direction of auditory motion in free field. A speaker array was used to generate horizontal and vertical motion sweeps crossing through the RF of recording sites (see Material and Methods). Moving sounds started 40 deg away from the RF center and traversed an angular distance of 80 deg; the second stimulus swept through the same line of speakers but in the opposite direction (Fig. 4A). The total stimulus duration was 0.5 s, resulting in an angular velocity of 160 deg/s. For horizontal motion, the firing rate increased when the stimulus entered the RF moving in both directions (Fig. 4B). The spatial tuning computed from average responses to the first stimuli after the direction switched (deviant) and the last trials before the switch (common) was similar (Fig. 4C and D). Notably, a shift in preferred location in the direction of the incoming sound was also observed for free-field stimulation (Fig. 4C and D).

The above results were consistent across the sample. Neurons showed no significantly different responses to the first stimulus in the block compared to the average response to the last stimuli in the

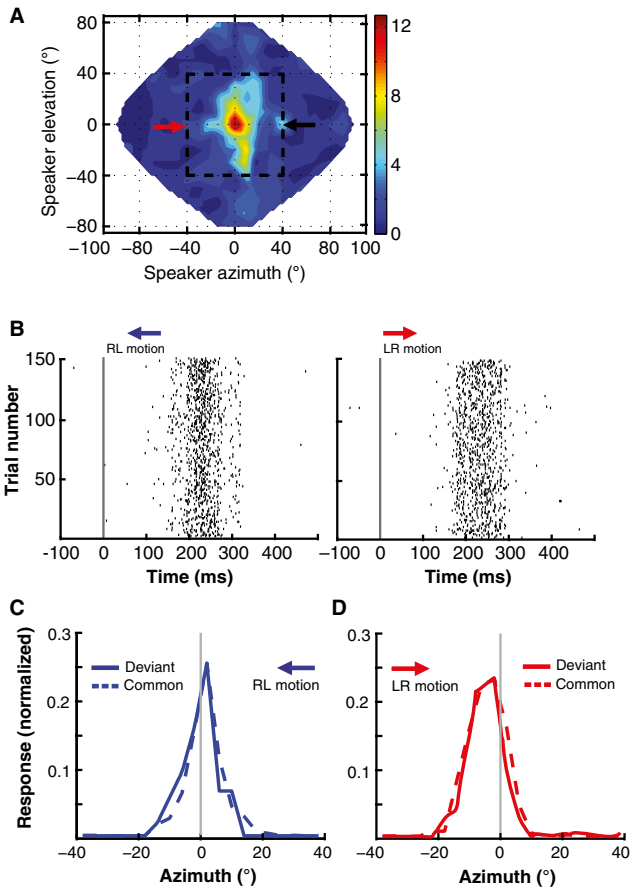

FIG. 4. Responses to motion in a constant order paradigm with stimuli presented in free field. (A) Spatial RF of a recording site. Color represents the average response to sound bursts from 144 speakers in the frontal hemifield (red corresponds to the highest response and blue the lowest). The dashed rectangle indicates the 7 by 7 speaker subset (covering 80 deg in azimuth and elevation) that was used for the motion sweeps. Red and black arrows indicate motion onset points of LR and RL motion sweeps, respectively. Motion ended at the start point of the stimulus moving in the opposite direction. (B) Raster plots of 150 trials of moving sound showing responses from the recording site whose RF is shown in A. On the left RL sweeps and on the right LR sweeps. The vertical lines indicate the onset of motion. (C) Average response as a function of azimuthal position of the speaker. The solid line represents the response to deviant stimuli and the dashed line to common stimuli. The vertical gray line designates the center of the static RF. (D) Same as in C but for the opposite motion direction.

block (Fig. 5A; $n = 104$, Wilcoxon signed rank test, $P = 0.72$ and $P = 0.06$, for right to left and left to right motion, respectively). The SI indices were not significantly biased above the diagonal lines (Fig. 5B; sign test, $P = 0.769$). In 58 recording sites, we performed a test where stimuli moving in opposite directions differed also in elevation (one stimulus was swept 10 deg above the center of the RF and the other stimulus 10 deg below the center of the RF). In this case, the average response to the first stimulus in each direction was significantly larger than the average response to the last stimuli (Fig. 5C; Wilcoxon signed rank test, $P = 0.003$ and $P < 0.001$, for right to left and left to right motion, respectively) and most of the data points in the SI scatterplot were significantly above the diagonal line (Fig. 5D; sign test, $P = 0.002$).

SSA was also tested in free field for vertical motion. Sounds moved up and down at a velocity of 160 deg/s through the same path, crossing the center of the RF. No significant SSA to the

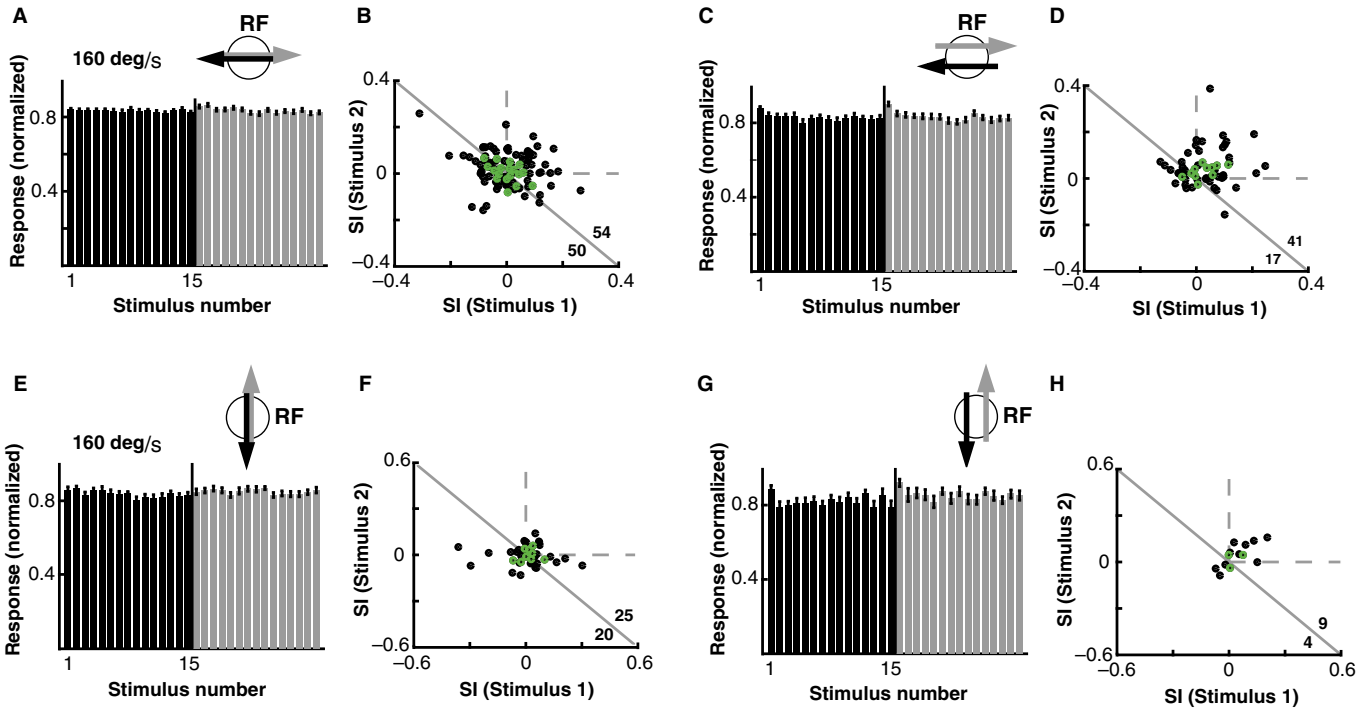

FIG. 5. Responses to free-field motion. (A) Average responses to horizontal motion in free field. The histogram shows average responses as a function of the order of the stimulus within the sequence. Black columns represent responses to leftward motions and gray columns to the opposite direction. In this experiment, the path in one direction overlapped with the path of the other direction (see inset). (B). SIs for one direction plotted vs. the SIs for the opposite direction. Dashed lines indicate the upper right quadrant. Gray dots represent results from single-unit recordings, black dots from multi-unit recordings. The number of points above and below the diagonal line are indicated in the lower right corner. (C) Average response to horizontal free-field motion where the two motion paths differed vertically (see inset in C). Same format as in A. (D) SIs for one direction vs. SIs for the other direction in the sample where the two motion paths differed vertically. Format as in B. (E) Average responses to vertically moving stimuli in both directions through the center of the RF (see inset). Black bars show the responses in the 15 trials of downward motion followed by the responses in the 15 trials of upwards motion (gray bars). Same format as in A. (F) SIs for upward motions vs. SIs for downwards motion. Same format as in B. (G) Average responses to vertically moving stimuli in two parallel paths (see inset). Same format as in A. (H) SIs for upward motion vs. SIs for downward motion when the upward and downward motions differed horizontally. Same format as in B.

direction of motion was observed (Fig. 5E and F, $n = 45$, Wilcoxon signed rank test, $P = 0.07$ and $P = 0.9$). In 13 recording sites, vertical motion in each direction was presented along two horizontally separated paths. In these cases, responses tended to display SSA, i.e., the population average responses to the first stimuli were larger compared to the average of the last three responses (Fig. 5G) but it did not reach statistical significance ($n = 13$; Wilcoxon signed rank test, $P = 0.07$ and $P = 0.08$). Because of the small number of experiments performed, this last result should be taken cautiously. However, it is consistent with the results from dichotic stimulation using ILD sweeps differing in ITD (Fig. 2K), Overall, the results from the free-field experiments indicate that tectal neurons do not show SSA to auditory motion direction in free field, consistent with the findings using sweeps in ITD and ILD.

SSA to the direction of a moving visual stimulus

Most neurons in the intermediate layers of OT of barn owls respond to both visual and auditory stimuli (Knudsen, 1982). We thus examined SSA to the direction of visual motion in these neurons using an equivalent paradigm to that used for auditory motion. Consistent with auditory responses, firing increased when the visual stimulus crossed the RF center and about the same magnitude of response was observed for both LR and RL motion (Fig. 6A and B). Also consistent with auditory responses, the spatial tuning for moving visual objects was shifted in the direction of the coming stimulus (Fig. 6C and D). However, unlike for auditory motion, the average response to the first stimuli in a sequence (Fig. 6C and D**;** solid lines) was larger than the average response to the last three stimuli in a sequence, for both directions (Fig. 6C and D; dashed lines). SSA to visual motion direction was significant at the population level, when the stimuli traveled the same path in opposite directions. At a stimulus velocity of 60 deg/s, the average responses to the first stimuli were larger than the average responses to the last three stimuli (Fig. 6E; $n = 40$, Wilcoxon signed rank test, $P < 0.001$ and $P < 0.001$, for right to left and left to right motion, respectively). The scatterplot shows a significant tendency of SIs to lay above the diagonal line (right panel in Fig. 6E; sign test, $P < 0.001$), indicating SSA. When the two stimuli moving horizontally differed in their vertical position (one moving along a path 5 deg above the center of the RF and the other 5 deg below the center of the RF), the SSA was stronger (compare Fig. 6F with Fig. 6E).

We performed the above experiments using two additional velocities (30 deg/s and 120 deg/s, Fig. 7A and B, respectively), as well as vertical motion at a velocity of 30 deg/s (Fig. 7C). In all cases, the average response to the first stimulus within a block was larger from the average response to the last three stimuli. This difference was significant in both directions (Fig. 7A, $n = 54$, Wilcoxon signed rank test, $P < 0.001$ and $P < 0.001$; Fig. 7B, $n = 52$, Wilcoxon signed rank test, $P = 0.001$ and $P < 0.001$; Fig. 7C, $n = 36$, Wilcoxon signed rank test, $P < 0.001$ and $P = 0.002$). In all three

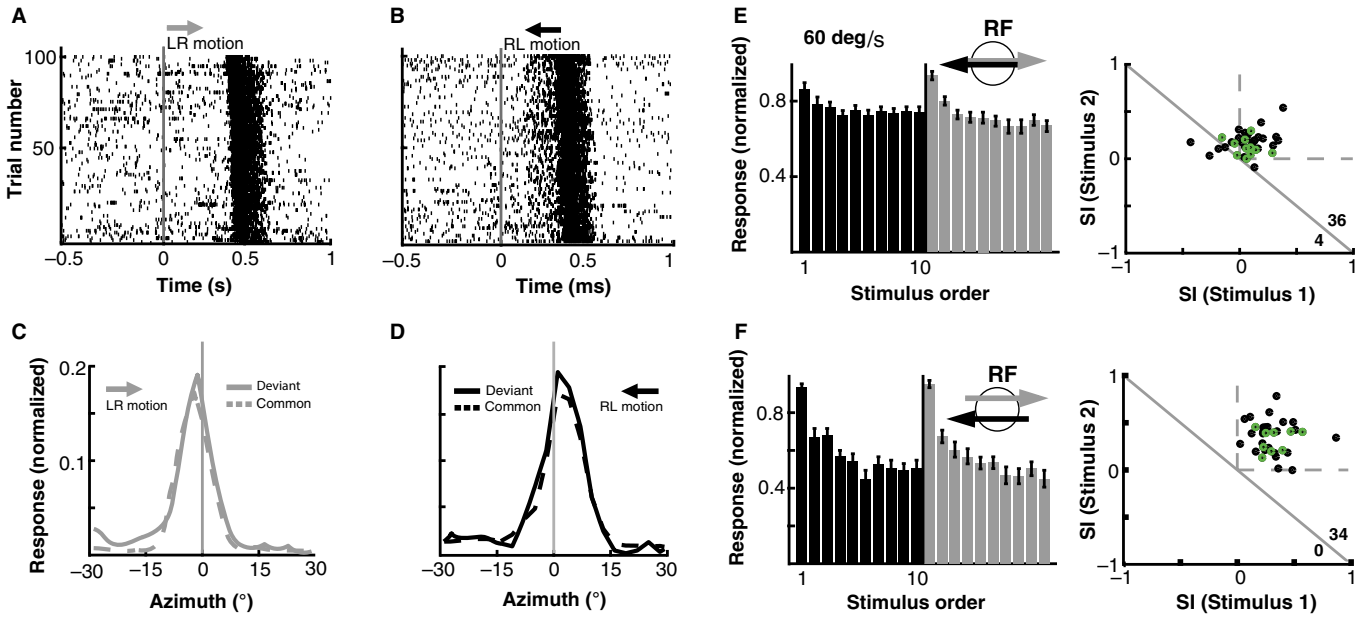

FIG. 6. SSA for visual motion. (A) Raster plot of responses to 100 trials of a visual stimulus moving rightward at 60 deg/s. The vertical line indicates the onset of the moving stimulus in time. The stimulus started 30 degrees left of the RF center and ended 30 degrees to the right. (B) Same as in A but for leftward motion. C) Average response as a function of the stimulus instantaneous location during rightward motion. The solid and dashed lines represent responses to the first (deviant) and last three (common) stimuli in each block, respectively. The vertical gray line represents the best azimuth measured for this site. (D) Same as in C except representing responses for leftward motions. (E) Average response across recording sites. The histogram shows responses as a function of the order of the stimulus within each block. Black bars represent responses to 10 leftward motions and gray bars to 10 rightward motions. Paths in both directions overlapped vertically (see inset). The scatterplot on the right shows the SIs for one direction plotted vs. the SIs for the opposite direction. Dashed lines indicate the upper right quadrant. Gray dots represent results from single-unit recordings, black dots from multi-unit recordings. The numbers in the lower right corner indicate the number of points above and below the diagonal line. (F) Results across the sample of recording sites in experiments where the paths in each direction differed vertically (see inset). Format as in E.

cases, the magnitude of the SSA increased when the two stimuli moved in parallel paths, separated either vertically (Fig. 7D and E) or horizontally (Fig. 7F). Thus, unlike auditory responses, visual responses showed robust SSA to motion direction as well as to position.

Discussion

This study compared SSA of auditory and visual motion in audio-visual neurons of the owl's OT. Each hemisphere of the map of auditory space in the barn owl's OT represents the frontal and contralateral space (Knudsen, 1982). The spatial tuning of tectal cells results from the integration of binaural (Moiseff & Konishi, 1983; Pena & Konishi, 2001) and spectral (Gold & Knudsen, 1999; Spezio & Takahashi, 2003; Cazettes *et al.*, 2014) cues. It has been argued that this elaborated computational process permits the alignment of auditory and visual spatial information, permitting multisensory integration and saliency mapping (Knudsen & Brainard, 1995; Gutfreund, 2012; Gutfreund & King, 2012). Indeed, spatial selectivity of auditory responses is remarkably consistent with visual responses in the OT. Both auditory and visual maps display a "frontal expansion" (Knudsen, 1982; Fischer & Pena, 2011). In addition, both modalities show similar patterns of lateral inhibition and cross-modal interactions (Mysore *et al.*, 2010), are modulated similarly by top–down connections (Winkowski & Knudsen, 2007) and display rapid SSA to the stimulus location (Reches & Gutfreund, 2008). These remarkable similarities support the view of OT as a hub for multisensory, context-dependent, integration (Gutfreund, 2012). Thus, despite the differences between visual and auditory representations at sub tectal levels, the representation of space at the OT displays similarities. However, this study has uncovered an inconsistency between auditory and visual representations in the OT of barn owls. Namely, visual responses displayed SSA to the direction of moving stimuli while auditory responses did not. This finding may reflect a fundamental difference between how the brain processes auditory and visual motion.

SSA is believed to result from synaptic depression or other cellular mechanisms underlying adaptation to excitation in pathways upstream the recorded neurons (Eytan *et al.*, 2003). If specific stimuli activate separate input pathways of an integrator neuron (for example each frequency channel of a neuron that integrates across frequency) and each input can undergo adaptation, stimulus-specific adaptation is expected at the integrator neuron (Duque *et al.*, 2016). This basic model has been further modified in recent studies to explain deviance detection (Taaseh *et al.*, 2011; Nelken, 2014). Thus, SSA can be used to elucidate the network architecture underlying neural representations. If SSA is observed for a sensory feature, it is likely that different states of this feature are carried by separate input pathways, allowing the specific adaptation. Thus, the observation that tectal neurons show SSA to the direction of visual motion suggests that this feature is explicitly encoded. Indeed, in the visual system, motion is believed to be encoded already in the retina (Barlow & Hill, 1963; Wei *et al.*, 2011), and is observed all along downstream pathways (Albright, 1984; Mikami *et al.*, 1986; Borst & Euler, 2011; Cruz-Martin *et al.*, 2014). In the OT, most neurons are only weakly sensitive to the direction of visual motion (Hughes & Pearlman, 1974; Knudsen, 1982). Thus, the robust SSA to the direction of visual motion reported here indicates that OT neurons are more sensitive to change in motion direction than to the

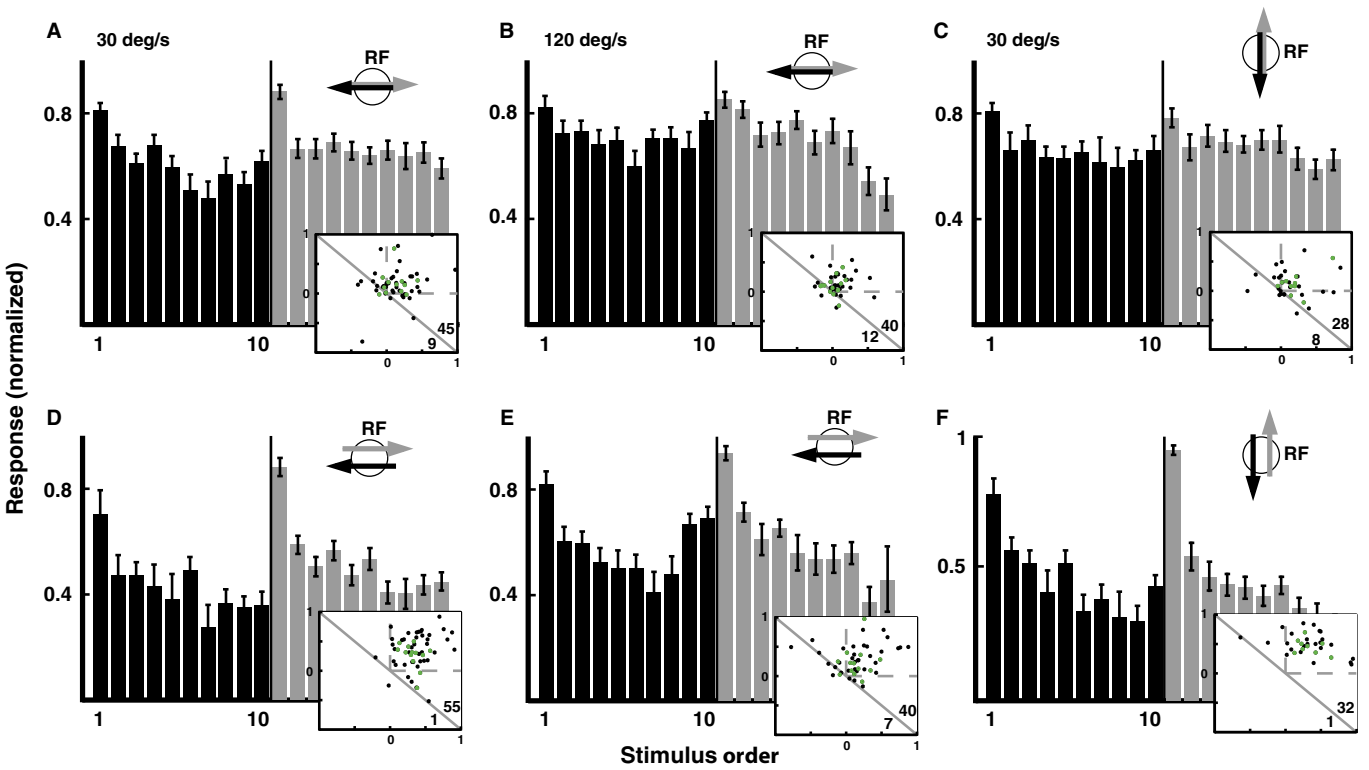

FIG. 7. Pooled responses to visual horizontal and vertical motion. (A) Average responses to horizontal motion at 30 deg/s, along the same path in both directions. Responses are sorted by trial order in the block. Black and gray bars indicate responses to leftward and rightward motion, respectively. The error bars indicate s.e.m. The inset shows the SIs for one direction vs. the SIs for the opposite direction. Gray dots represent results from single-unit recordings, black dots from multi-unit recordings. The numbers in the lower right corner of the inset indicate the number of points above and below the diagonal line. (B) Average responses to horizontal motion (120 deg/s) along the same path in both directions. Same format as in A. (C) Average responses to vertical motion (30 deg/s). Black and gray bars indicate responses to downward and upward motion, respectively. The paths of both stimuli overlap horizontally. Same format as in A. (D) Average responses as a function of order of the trial within the block for horizontal motion (30 deg/s) along paths separated in elevation (see inset). Same format as in A. (E) Average responses as a function of order of the trial within the block for horizontal motion (120 deg/s) along paths separated in elevation (see inset). Same format as in A. (F) Average responses as a function of trial order in the block for vertical motion (30 deg/s) along paths separated in azimuth (see inset). Same format as in A.

direction of motion itself, a property consistent with their suggested role in saliency detection.

In contrast to visual motion, no SSA was observed here for auditory motion direction. Because SSA may depend on stimulus parameters and stimulation paradigm, we tested two velocities, two paradigms (constant order and oddball) and three types of methods to mimic motion (ITD and ILD sweeps and motion in free field), all failing to induce SSA. On the other hand, in control experiments using the same paradigms but separating motion paths, SSA was consistently observed. Thus, our results suggest that the lack of SSA to acoustic motion direction is likely a fundamental property of tectal neurons in barn owls. This claim does not rule out the possibility that SSA to acoustic motion direction is present elsewhere in the brain. However, given the findings that tectal neurons show significant SSA to practically any auditory feature tested so far: ITD, ILD, frequency and intensity (Reches & Gutfreund, 2008) as well as complex sounds (Netser *et al.*, 2011), we hypothesize that the lack of motion SSA reflects the lack of circuitry dedicated to auditory motion direction in the early auditory pathway. This constitutes a remarkable difference with the visual pathway.

Sensitivity to auditory motion direction has been reported in the owl's external nucleus of the inferior colliculus (ICx) (Wagner & Takahashi, 1992; Wang *et al.*, 2012, 2014), the main source of auditory input to OT. Recently, (Wang & Pena, 2013) demonstrated that directional selectivity in the ICx can be explained by adaptation to excitation in asymmetrical spatial receptive fields. Similarly, McAlpine *et al.* (2000) suggested that adaptation to excitation can account for most of the auditory directional selectivity in the mammalian inferior colliculus. Thus, direction selectivity to auditory motion in single neurons, however necessary, is not sufficient to demonstrate the existence of a dedicated pathway for acoustic motion. The presence of adaptation together with lateral inhibition, may explain another notable difference between responses to opposing motion directions, namely, moving sounds elicit a shift in spatial tuning toward the direction of the incoming stimulus (Witten *et al.*, 2006). In the OT, this phenomenon had only been reported for ITD sweeps before (Witten *et al.*, 2006). Here, we extend this observation to sounds moving in free field (Fig. 4C and D) as well as in visual motion (Fig. 6C and D).

Psychophysical studies in humans show an auditory motion aftereffect (aMAE), where prolonged exposure to sounds moving in one direction induces a perceptual bias for the opposite direction (Grantham, 1989; Dong *et al.*, 2000; Neelon & Jenison, 2004). The aMAE is reminiscent, albeit weaker, of the waterfall aftereffect (Ehrenstein, 1994) and has been advanced as indicating dedicated processing of auditory motion (Dong *et al.*, 2000). However, auditory evoked potentials recorded in subjects during the same conditions that induced an aMAE could not detect specific adaptation to the direction of auditory motion (Magezi *et al.*, 2013). Thus, it is yet to be determined if the human aMAE results

from adaptation in processing pathways dedicated specifically to motion direction or a different mechanism (Boucher *et al.*, 2004). A recent study in barn owls investigated behavioral sensitivity to the direction of auditory motion (Langemann *et al.*, 2016). It was shown that to discriminate motion direction, the angular range of motion was required to be larger than 20 deg which is considerably larger than the owl's minimum audible angle (Bala *et al.*, 2007). The authors interpret this finding as a support against the "snapshot" hypothesis (Langemann *et al.*, 2016). However, others have argued that the relatively large angular range that is necessary also for humans to discriminate sound direction does not support a dedicated sound direction processing circuitry (Middlebrooks & Green, 1991).

It is generally accepted that neurons selective to the direction of auditory motion are relatively rare, weakly tuned, or emerge from history-dependent firing properties of the recorded neurons (Altman, 1968; Kuwada *et al.*, 1979; Yin & Kuwada, 1983; McAlpine *et al.*, 2000; Ingham *et al.*, 2001; McAlpine & Palmer, 2002; Wang & Pena, 2013). This is in marked contrast to the visual system where motion parameters are commonly and robustly represented (Maunsell & Van Essen, 1983; Albright, 1984). The current study is the first to compare directly between visual and auditory motion processing in the same population of neurons and using the same paradigms. The findings are consistent with the hypothesis that there are fundamental differences in how motion is processed in the two modalities. We hypothesize that this difference is general across species, due to the higher computational demands for spatial processing in the auditory system.

Conflict of interest

The authors declare no competing financial interests or any other conflict of interest.

Acknowledgement

This work was supported by a grant from the Binational Science Foundation to YG and JLP, a grant from the Israel Science Foundation to YG, an Adelis Research Foundation grant to YG and an NIH grant number DC007690 to JLP.

Data accessibility

Raw data supporting this article can be received by e-mail upon request.

References

Albright, T.D. (1984) Direction and orientation selectivity of neurons in visual area MT of the macaque. *J. Neurophysiol.*, **52**, 1106–1130.

Altman, J.A. (1968) Are there neurons detecting direction of sound source motion? *Exp. Neurol.*, **22**, 13–25.

Anstis, S., Verstraten, F.A. & Mather, G. (1998) The motion aftereffect. *Trends Cogn Sci.*, **2**, 111–117.

Bala, A.D., Spitzer, M.W. & Takahashi, T.T. (2007) Auditory spatial acuity approximates the resolving power of space-specific neurons. *PLoS ONE*, **2**, e675.

Barlow, H.B. & Hill, R.M. (1963) Selective sensitivity to direction of movement in ganglion cells of the rabbit retina. *Science*, **139**, 412–414.

Borst, A. & Euler, T. (2011) Seeing things in motion: models, circuits, and mechanisms. *Neuron*, **71**, 974–994.

Boucher, L., Lee, A., Cohen, Y.E. & Hughes, H.C. (2004) Ocular tracking as a measure of auditory motion perception. *J. Physiol. Paris*, **98**, 235–248.

Brainard, D.H. (1997) The psychophysics toolbox. *Spat. Vis.*, **10**, 433–436.

Brainard, M.S. & Knudsen, E.I. (1993) Experience-dependent plasticity in the inferior colliculus: a site for visual calibration of the neural representation of auditory space in the barn owl. *J. Neurosci.*, **13**, 4589–4608.

Cazettes, F., Fischer, B.J. & Pena, J.L. (2014) Spatial cue reliability drives frequency tuning in the barn Owl's midbrain. *Elife*, **3**, e04854.

Cruz-Martin, A., El-Danaf, R.N., Osakada, F., Sriram, B., Dhande, O.S., Nguyen, P.L., Callaway, E.M., Ghosh, A. *et al.* (2014) A dedicated circuit links direction-selective retinal ganglion cells to the primary visual cortex. *Nature*, **507**, 358–361.

Dong, C.J., Swindale, N.V., Zakarauskas, P., Hayward, V. & Cynader, M.S. (2000) The auditory motion aftereffect: its tuning and specificity in the spatial and frequency domains. *Percept. Psychophys*, **62**, 1099–1111.

Duque, D., Wang, X., Nieto-Diego, J., Krumbholz, K. & Malmierca, M.S. (2016) Neurons in the inferior colliculus of the rat show stimulus-specific adaptation for frequency, but not for intensity. *Sci. Rep.*, **6**, 24114.

Ehrenstein, W.H. (1994) Auditory aftereffects following simulated motion produced by varying interaural intensity or time. *Perception*, **23**, 1249–1255.

Eytan, D., Brenner, N. & Marom, S. (2003) Selective adaptation in networks of cortical neurons. *J. Neurosci.*, **23**, 9349–9356.

Fischer, B.J. & Pena, J.L. (2011) Owl's behavior and neural representation predicted by Bayesian inference. *Nat. Neurosci.*, **14**, 1061–1066.

Gold, J.I. & Knudsen, E.I. (1999) Hearing impairment induces frequency-specific adjustments in auditory spatial tuning in the optic tectum of young owls. *J. Neurophysiol.*, **82**, 2197–2209.

Gold, J.I. & Knudsen, E.I. (2000) A site of auditory experience-dependent plasticity in the neural representation of auditory space in the barn owl's inferior colliculus. *J. Neurosci.*, **20**, 3469–3486.

Grantham, D.W. (1986) Detection and discrimination of simulated motion of auditory targets in the horizontal plane. *J. Acoust. Soc. Am.*, **79**, 1939–1949.

Grantham, D.W. (1989) Motion aftereffects with horizontally moving sound sources in the free field. *Percept. Psychophys*, **45**, 129–136.

Gutfreund, Y. (2012) Stimulus-specific adaptation, habituation and change detection in the gaze control system. *Biol. Cybern.*, **106**, 657–668.

Gutfreund, Y. & King, A.J. (2012) What is the role of vision in the development of the auditory space map? In Stein, B.E. (Ed.), *The new Handbook of Multisensory Processing*. The MIT press, Cambridge, MA, pp. 573–588.

Hughes, C.P. & Pearlman, A.L. (1974) Single unit receptive fields and the cellular layers of the pigeon optic tectum. *Brain Res.*, **80**, 365–377.

Ingham, N.J., Hart, H.C. & McAlpine, D. (2001) Spatial receptive fields of inferior colliculus neurons to auditory apparent motion in free field. *J. Neurophysiol.*, **85**, 23–33.

Keller, C.H., Hartung, K. & Takahashi, T.T. (1998) Head-related transfer functions of the barn owl: measurement and neural responses. *Hear. Res.*, **118**, 13–34.

Knudsen, E.I. (1982) Auditory and visual maps of space in the optic tectum of the owl. *J. Neurosci.*, **2**, 1177–1194.

Knudsen, E.I. & Brainard, M.S. (1995) Creating a unified representation of visual and auditory space in the brain. *Annu. Rev. Neurosci.*, **18**, 19–43.

Kuwada, S., Yin, T.C. & Wickesberg, R.E. (1979) Response of cat inferior colliculus neurons to binaural beat stimuli: possible mechanisms for sound localization. *Science*, **206**, 586–588.

du Lac, S. & Knudsen, E.I. (1990) Neural maps of head movement vector and speed in the optic tectum of the barn owl. *J. Neurophysiol.*, **63**, 131–146.

Langemann, U., Krumm, B., Liebner, K., Beutelmann, R. & Klump, G.M. (2016) Moving objects in the Barn Owl's auditory world. In Van Dijk, P., Başkent, D., Gaudrain, E., De Kleine, E., Wagner, A. & Lanting, C. (Eds), *Physiology, Psychoacoustics and Cognition in Normal and Impaired Hearing*. Springer International Publishing, New York, NY, pp. 219–227.

Magezi, D.A., Buetler, K.A., Chouiter, L., Annoni, J.M. & Spierer, L. (2013) Electrical neuroimaging during auditory motion aftereffects reveals that auditory motion processing is motion sensitive but not direction selective. *J. Neurophysiol.*, **109**, 321–331.

Malmierca, M.S., Cristaudo, S., Perez-Gonzalez, D. & Covey, E. (2009) Stimulus-specific adaptation in the inferior colliculus of the anesthetized rat. *J. Neurosci.*, **29**, 5483–5493.

Maunsell, J.H. & Van Essen, D.C. (1983) Functional properties of neurons in middle temporal visual area of the macaque monkey. I. Selectivity for stimulus direction, speed, and orientation. *J. Neurophysiol.*, **49**, 1127–1147.

McAlpine, D. & Palmer, A.R. (2002) Blocking GABAergic inhibition increases sensitivity to sound motion cues in the inferior colliculus. *J. Neurosci.*, **22**, 1443–1453.
McAlpine, D., Jiang, D., Shackleton, T.M. & Palmer, A.R. (2000) Responses of neurons in the inferior colliculus to dynamic interaural phase cues: evidence for a mechanism of binaural adaptation. *J. Neurophysiol.*, **83**, 1356–1365.
Middlebrooks, J.C. (2015) Sound localization. *Handb. Clin. Neurol.*, **129**, 99–116.
Middlebrooks, J.C. & Green, D.M. (1991) Sound localization by human listeners. *Annu. Rev. Psychol.*, **42**, 135–159.
Mikami, A., Newsome, W.T. & Wurtz, R.H. (1986) Motion selectivity in macaque visual cortex. I. Mechanisms of direction and speed selectivity in extrastriate area MT. *J. Neurophysiol.*, **55**, 1308–1327.
Moiseff, A. (1989) Bi-coordinate sound localization by the barn owl. *J. Comp. Physiol. A.*, **164**, 637–644.
Moiseff, A. & Konishi, M. (1983) Binaural characteristics of units in the owl's brainstem auditory pathway: precursors of restricted spatial receptive fields. *J. Neurosci.*, **3**, 2553–2562.
Mysore, S.P., Asadollahi, A. & Knudsen, E.I. (2010) Global inhibition and stimulus competition in the owl optic tectum. *J. Neurosci.*, **30**, 1727–1738.
Neelon, M.F. & Jenison, R.L. (2004) The temporal growth and decay of the auditory motion aftereffect. *J. Acoust. Soc. Am.*, **115**, 3112–3123.
Nelken, I. (2014) Stimulus-specific adaptation and deviance detection in the auditory system: experiments and models. *Biol. Cybern.*, **108**, 655–663.
Netser, S., Ohayon, S. & Gutfreund, Y. (2010) Multiple manifestations of microstimulation in the optic tectum: eye movements, pupil dilations, and sensory priming. *J. Neurophysiol.*, **104**, 108–118.
Netser, S., Zahar, Y. & Gutfreund, Y. (2011) Stimulus-specific adaptation: can it be a neural correlate of behavioral habituation? *J. Neurosci.*, **31**, 17811–17820.
Newsome, W.T. & Pare, E.B. (1988) A selective impairment of motion perception following lesions of the middle temporal visual area (MT). *J. Neurosci.*, **8**, 2201–2211.
Olsen, J.F., Knudsen, E.I. & Esterly, S.D. (1989) Neural maps of interaural time and intensity differences in the optic tectum of the barn owl. *J. Neurosci.*, **9**, 2591–2605.
Pena, J.L. & Konishi, M. (2001) Auditory spatial receptive fields created by multiplication. *Science*, **292**, 249–252.
Perez, M.L., Shanbhag, S.J. & Pena, J.L. (2009) Auditory spatial tuning at the crossroads of the midbrain and forebrain. *J. Neurophysiol.*, **102**, 1472–1482 Epub 2009 Jul 1471.
Poganiatz, I. & Wagner, H. (2001) Sound-localization experiments with barn owls in virtual space: influence of broadband interaural level different on head-turning behavior. *J. Comp. Physiol. A.*, **187**, 225–233.
Poganiatz, I., Nelken, I. & Wagner, H. (2001) Sound-localization experiments with barn owls in virtual space: influence of interaural time difference on head-turning behavior. *J. Assoc. Res. Oto.*, **2**, 1–21.
Reches, A. & Gutfreund, Y. (2008) Stimulus-specific adaptations in the gaze control system of the barn owl. *J. Neurosci.*, **28**, 1523–1533.
Snowden, R.J. & Freeman, T.C. (2004) The visual perception of motion. *Curr. Biol.*, **14**, R828–R831.
Spezio, M.L. & Takahashi, T.T. (2003) Frequency-specific interaural level difference tuning predicts spatial response patterns of space-specific neurons in the barn owl inferior colliculus. *J. Neurosci.*, **23**, 4677–4688.
Taaseh, N., Yaron, A. & Nelken, I. (2011) Stimulus-specific adaptation and deviance detection in the rat auditory cortex. *PLoS ONE*, **6**, e23369.
Ulanovsky, N., Las, L. & Nelken, I. (2003) Processing of low-probability sounds by cortical neurons. *Nat Neurosci*, **6**, 391–398.
Ulanovsky, N., Las, L., Farkas, D. & Nelken, I. (2004) Multiple time scales of adaptation in auditory cortex neurons. *J. Neurosci.*, **24**, 10440–10453.
Wagner, H. & Takahashi, T. (1992) Influence of temporal cues on acoustic motion-direction sensitivity of auditory neurons in the owl. *J. Neurophysiol.*, **68**, 2063–2076.
Wang, Y. & Pena, J.L. (2013) Direction selectivity mediated by adaptation in the owl's inferior colliculus. *J. Neurosci.*, **33**, 19167–19175.
Wang, Y., Shanbhag, S.J., Fischer, B.J. & Pena, J.L. (2012) Population-wide bias of surround suppression in auditory spatial receptive fields of the owl's midbrain. *J. Neurosci.*, **32**, 10470–10478.
Wang, Y., Gutfreund, Y. & Pena, J.L. (2014) Coding space-time stimulus dynamics in auditory brain maps. *Front. Physiol.*, **5**, 135.
Wei, W., Hamby, A.M., Zhou, K. & Feller, M.B. (2011) Development of asymmetric inhibition underlying direction selectivity in the retina. *Nature*, **469**, 402–406.
Weigelt, S., Muckli, L. & Kohler, A. (2008) Functional magnetic resonance adaptation in visual neuroscience. *Rev. Neurosci.*, **19**, 363–380.
Winkowski, D.E. & Knudsen, E.I. (2007) Top-down control of multimodal sensitivity in the barn owl optic tectum. *J. Neurosci.*, **27**, 13279–13291.
Witten, I.B., Bergan, J.F. & Knudsen, E.I. (2006) Dynamic shifts in the owl's auditory space map predict moving sound location. *Nat. Neurosci.*, **9**, 1439–1445 Epub 2006 Oct 1431.
Yin, T.C. & Kuwada, S. (1983) Binaural interaction in low-frequency neurons in inferior colliculus of the cat. II. Effects of changing rate and direction of interaural phase. *J. Neurophysiol.*, **50**, 1000–1019.